

Powder X-ray Diffraction Basic Course

Second installment: Selection of equipment configuration to obtain high-quality data

Masashi Omori*

1. Introduction

It is necessary to obtain high-quality data for highly accurate analysis. The characteristics of high-quality data may be high intensity, high resolution, high P/B (peak-to-background ratio), and high S/N (signal-to-noise ratio). Deciding which features are important depends on the purpose of analysis. Therefore, we need to consider measurement conditions after determining the purpose of analysis. Some combinations of sample types and optical systems prevent the desired results from being obtained. Therefore, it is necessary to select the optical systems according to the kinds of samples.

The equipment configurations required to obtain high-quality data will be explained here and in the following articles in this powder X-ray diffraction basic course. The measurement conditions we will be discussing include selection of the equipment, sample preparation, and scan conditions. Selection of the equipment will be covered in this article, and sample preparation and scan conditions will be discussed in the third article.

The following sections in this article explore the factors involved in selecting the proper equipment configurations to obtain high-quality data: 2. Selection of X-ray source, 3. Selection of optical systems, 4. & 5. Setting incident and receiving optical systems, and 6. Detector configuration. These sections are arranged in order from the X-ray source to the receiving optical system.

2. Selection of X-ray Source

X-ray sources are defined by the following elements: (a) tube type, (b) type of target metal, and (c) type of focus. Each of these will be explained in the following sections.

(a) Structural differences

There are two types of X-ray sources: sealed X-ray tubes and rotating anode X-ray tubes. When copper is used as the target metal, the power of the sealed tube source will be approximately 2kW and that of the rotating anode X-ray tube will be 9kW for Rigaku's SmartLab X-ray diffractometer. Figure 1 shows the X-ray diffraction profiles of Si powder measured using a sealed tube and a rotating anode source. The power of the sealed tube was 40kV/50mA. The intensity measured using a rotating anode X-ray tube was 4.6

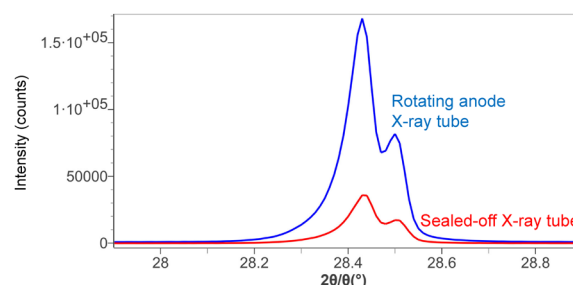


Fig. 1. X-ray diffraction profiles measured using a sealed X-ray tube and a rotating anode X-ray tube (Target metal: Cu, Sample: Si powder).

times higher than that measured using a sealed X-ray tube, which indicates that the measurement time can be reduced using a rotating anode X-ray tube.

(b) Kinds of target metal

The wavelength of the characteristic X-rays depends on the kind of metal used in the X-ray source (hereinafter called the target metal). Cr, Fe, Co, Cu, Mo, and Ag are commonly used as target metals in X-ray diffractometry. Table 1 shows the wavelength of the characteristic X-rays of each target metal. The wavelength of the characteristic X-rays ($K\alpha$ line) becomes shorter as the atomic number increases.

Table 1. Wavelength of the characteristic X-rays ($K\alpha$ line) of common target metals.

Element	Cr	Fe	Co	Cu	Mo	Ag
Atomic number	24	26	27	29	42	47
Wavelength (Å)	2.29	1.94	1.79	1.54	0.71	0.56

The wavelength of $CuK\alpha$ is 1.54 Å, which makes it suitable for measurements of general materials having lattice parameters of 1–10 Å. However, the suitable target metal also depends on the elements contained in the sample, as well as on the purpose of analysis. Table 2 summarizes the relationships between the purpose of analysis, the target metal, and major elements in samples.

The excitation voltage required to obtain the characteristic X-rays ($K\alpha$ line) is determined by the target metal. The maximum X-ray tube current is determined by the maximum allowed load of the X-ray

* Application Laboratories, Rigaku Corporation.

Table 2. Relationships of the purpose of analysis, target metal, and elements of the samples.

Purpose	Target metal	Major element in samples	Special notes
Qualitative Quantitative Structure	Cu	Ordinary	—
		Fe-based	<ul style="list-style-type: none"> Fluorescence X-ray reduction (XRF) mode Monochromator
		Ni-based	<ul style="list-style-type: none"> $K\beta$ filter on the incident optical side Optical system with divergence mirror (CBO-α)
	Co	Fe-based	<ul style="list-style-type: none"> $K\beta$ filter on the incident optical side CBO-α
	Fe	Fe-based	—
Residual stress	Cr Co	Fe	<ul style="list-style-type: none"> Pseudo-parallel beam method Parallel beam (PB) method
	Cu	Cu, Ni, Ceramics	PB method
Pair Distribution Function (PDF)	Mo Ag	Ordinary	The measurable wavenumber range of Ag is wider than that of Mo

diffractometer and X-ray tube. Incidentally, for a sealed X-ray tube, the lifetime of the X-ray tube is extended if used at no more than 90% of its maximum power output.

(c) Types of focus

Characteristic X-rays are generated by collisions of thermo-electrons generated by the filament with the target metal. The area generating characteristic X-rays on the target metal is called the real focus size.

There are three types of focuses in sealed X-ray tubes: normal focus (real focus size: 1×10mm), fine focus (0.4×8mm), and long fine focus (0.4×12mm). Figure 2 shows the comparison between diffraction profiles measured using normal and fine focus. The angular resolution of fine focus is better than that of normal focus because of the smaller real focus size. The real focus size in the longitudinal direction of the long fine focus is longer than that of other focus types. In order not to block the incident X-rays, it is preferable to use a 15mm longitudinal slit. Furthermore, the real focus size of 0.4×8mm of the rotating anode X-ray tube is the same as that of the fine focus sealed tube.

3. Selection of Optical Systems

The difference between the reflection method and transmission method is the arrangements of the X-ray source, sample, and detector. Figure 3 shows schematic diagrams of the reflection and transmission methods. The reflection method is used for measurements of powder samples filled in sample holders or bulk-shaped samples. On the other hand, the transmission method

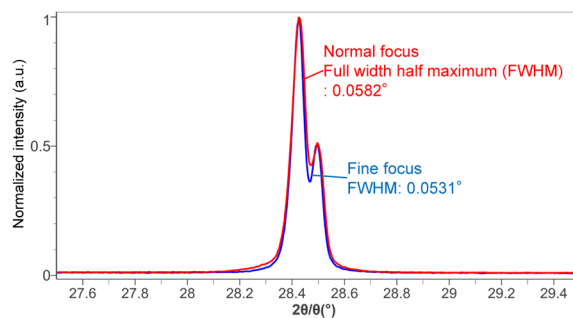


Fig. 2. Profiles measured by normal focus and fine focus (Target metal: Cu, Sample: Si powder).

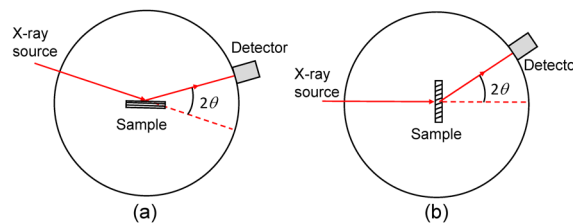


Fig. 3. Schematic diagrams of the reflection method (a) and transmission method (b).

is selected for measurement of highly oriented powder samples or film-shaped samples.

The Bragg-Brentano para-focusing method (hereinafter called the “BB method”) or the parallel beam method (hereinafter called the “PB method”) are used for the reflection method. The PB method or focusing optical system at the detector (hereinafter called the “focusing beam method”) is used for the transmission method. An ellipsoidal multilayer mirror (CBO-E) is used for the focusing beam method. The advantages of and cautionary notes for each optical system are summarized as follows.

Bragg-Brentano para-focusing method

- High peak intensity and resolution can easily be obtained.^{(1),(2)}
- The scan axis is limited to the 2θ/θ axis.
- Sample surface needs to be flat.

Parallel beam method

- Peak intensity and resolution depend on the width of the slit.
- Various scan axes are available.
- Samples with rough surfaces can be measured.
- In the case of a 0-dimensional scan, the peak intensity is lower than with the BB method.

Focusing beam method

- This method is only used for the transmission method.
- Compared to the PB method, high peak intensity and resolution can be obtained.

Various optical systems can be selected by changing the multilayer mirror. In the next section, how to set up the incident and receiving optical system is explained.

4. Bragg–Brentano para-Focusing Method

4.1. Monochromatization

In the case of the BB method, it is necessary to reduce unnecessary characteristic X-rays ($K\beta$ line) using either the incident or receiving optical system. These methods are used to reduce the $K\beta$ line on the receiving side: (a) $K\beta$ filter method and (b) monochromator method. To reduce the $K\beta$ line on the incident side, (c) the method using the divergence mirror will be discussed.

(a) $K\beta$ filter method

In the $K\beta$ filter method, $K\beta$ lines are reduced with a thin film of metal. This method is widely used for BB method measurements and is inexpensive because monochromators and mirrors are not required. Moreover, compared to the monochromator method, higher peak intensity can be obtained. The $K\beta$ filter strongly attenuates a limited range of wavelengths; therefore, fluorescent X-rays generated from the sample may penetrate the $K\beta$ filter, which will make the background level higher. These fluorescent X-rays can be reduced using the fluorescent X-ray reduction mode (see below). For the purpose of further background reduction, it is necessary to consider using the monochromator method and the method using a divergence mirror.

(b) Monochromator method

In this method, the objective wavelength ($K\alpha$ line) is selected using the spectroscopy of the graphite crystals. The wavelength resolution of this method is higher than that of the $K\beta$ filter method; therefore, fluorescent X-rays can be reduced. It is particularly effective for the measurement of Fe-based samples with a Cu target. Moreover, continuous X-rays can also be reduced and, as a result, high P/B ratio can be obtained. However, when the sample includes the same element as the target metal, the fluorescent X-rays of the sample cannot be reduced. It should be noted that the intensity of the diffracted X-rays in the monochromator method is lower than that of the $K\beta$ filter method; therefore, the measurement requires a longer time to achieve similar results.

There are two types of monochromators: one for one-dimensional (1D) measurement and the other for zero-dimensional (0D) measurement. The intensity of the profile measured with the monochromator for 1D measurement is 40 times higher than that for 0D measurement. However, the energy resolution of the monochromator for 1D measurement is inferior to that for 0D measurement, therefore $K\beta$ lines with 0.2% relative intensity to the $K\alpha$ lines are detected.

(c) The method using divergence mirror⁽³⁾

Monochromatic X-rays can be irradiated onto the sample using a plane multilayer mirror (CBO- α). This method is effective in cases where the sample generates fluorescent X-rays due to irradiation from other than the $K\alpha$ line. This applies to the measurements of Ni-based or Cu-based samples using a Cu target, and of Fe-based samples using a Co target.⁽⁴⁾ Furthermore, because a $K\beta$ filter is not used, the absorption edge of the filter has

no effect on the measured profile. Moreover, because monochromatic X-rays are irradiated onto the sample, fluorescent X-rays can be reduced and low background data can be obtained compared to the $K\beta$ filter method. The intensity ratio of $K\alpha$ and $K\beta$ lines is 500:1 and the intensity of the $K\beta$ line can be further reduced by a combination of CBO- α and $K\beta$ filter method. This method is used for the detection of minute peaks.

The maximum angles of the divergence slit of the sealed X-ray tube and rotating anode X-ray tube are $1/2^\circ$ and $1/3^\circ$, respectively. The incident slit needs to be selected below these values.

4.2. Selection of incident and receiving optical system

In the BB method, the focal point of the X-ray tube and the detection area of the detector are aligned on a circle centered at the sample position. The radius of the circle is called the goniometer radius. As the goniometer radius increases, the angular resolution increases and the diffraction intensity decreases. Generally, the goniometer radius of a desktop type X-ray diffractometer is approximately 150 mm and that of a stationary type X-ray diffractometer is approximately 300 mm. The goniometer radius is determined by the type of the equipment and cannot be optimized. However, the incident and receiving optical systems must be optimized according to the sample.

Figure 4 shows an example of a schematic diagram of the BB method. X-rays are generated from the X-ray tube and pass the (a) incident soller slit, (b) incident slit, and (c) longitudinal slit. Then, X-rays are irradiated onto the sample. Diffracted X-rays pass the (e) receiving soller slit, (f) $K\beta$ filter, (g) receiving soller slit, (h) receiving slit 2, and attenuator and are detected on the detector. The (d) scattering protector or knife edge is used to block scattered X-rays. The selection of each optical device is explained in the following sections.

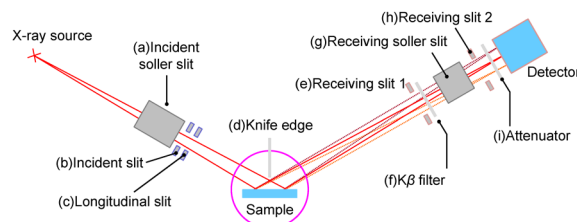


Fig. 4. Schematic diagram of the BB method.

(a) Incident soller slit

The incident solar slit is the slit used to suppress divergence in the direction vertical to the plane in Fig. 4 (hereinafter called the longitudinal direction). The irradiation width in the longitudinal direction is determined by both the incident soller slit and the longitudinal slit. When an incident solar slit with a small width is used, divergence of the irradiated area can be suppressed. On the other hand, diffraction intensity decreases and a longer measurement time is needed.

Furthermore, peak tailing (the umbrella effect) can be reduced using incident and receiving sollar slits that have small widths (described later).

(b) Incident slit

The divergence angle of the incident X-rays is determined by the incident slit and it alters the irradiation width. Figure 5 shows the relationship between the incident slit and irradiation width.

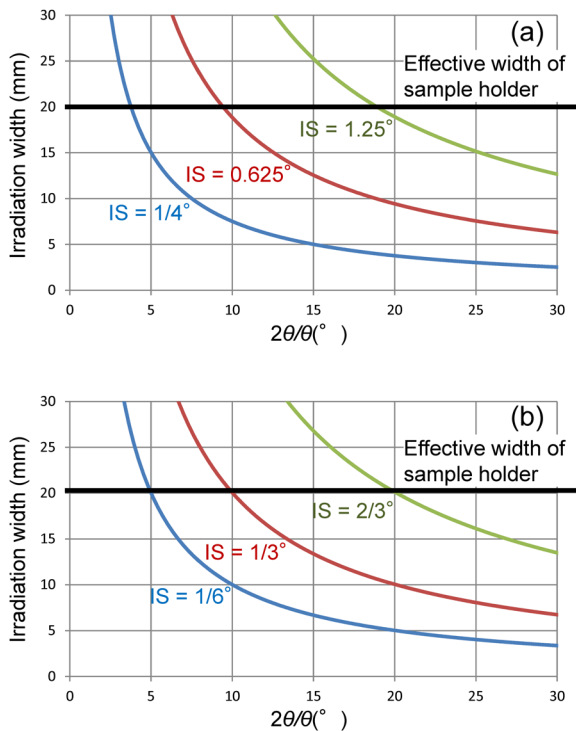


Fig. 5. Relationship between the incident slit and irradiation width Goniometer radius (a) 150 mm, (b) 300 mm.

As the incident angle decreases, the irradiation width increases. If the irradiation width is wider than the sample size, problems occur; for example, the intensity ratio of the peaks is wrong or diffraction from something other than the sample (such as the sample holder) is detected. The diffraction intensity depends on the width of the incident slit; therefore, to obtain high intensity and the correct peak intensity ratio, it is necessary to select the optimal incident slit such that the incident slit is as wide as possible while ensuring that the irradiation area is smaller than the sample size.

(c) Longitudinal slit

The longitudinal slit restricts the beam size in the longitudinal direction and determines the irradiation width in the longitudinal direction (longitudinal irradiation width). Table 3 shows the relationship between the incident sollar slit and longitudinal slit in the case of the SmartLab.

When incident X-rays irradiate the area outside the sample, diffraction from the sample holder is generated and profiles with high backgrounds can be obtained. Therefore, it is necessary to select the optimal longitudinal slit so that the irradiation area is kept smaller than the sample size.

Table 3. The relationship between the incident sollar slit and longitudinal slit (SmartLab)

Incident sollar slit	Longitudinal slit	Longitudinal irradiation width (Measured value)
5.0°	10 mm	19 mm
	5 mm	13 mm
	2 mm	10 mm
2.5°	10 mm	14 mm
	5 mm	9 mm
	2 mm	6 mm

(d) Scattering protector, knife edge

One cause of high backgrounds is scattering from air or slits. The background in measurements using 1D detectors tends to be higher than that using 0D detectors because of the wide receiving slit.

In order to block the scattered X-rays, installation of a scattering protector or knife edge is considered.⁽⁵⁾ In some situations, a scattering prevention tube is used instead of a scattering protector. Figure 6 shows the profile with and without the scattering protector and knife edge.

When a scattering protector and knife edge are not used, scattering is detected below $2\theta=40^\circ$. On the other hand, when a scattering protector or knife edge is used, scattering decreases. However, when a knife edge is used, the peak intensity derived from Si powder may decrease on the high angle side because the knife edge blocks the diffracted X-rays. Therefore, the knife edge is effective in the case of measurement below $2\theta=70^\circ$,

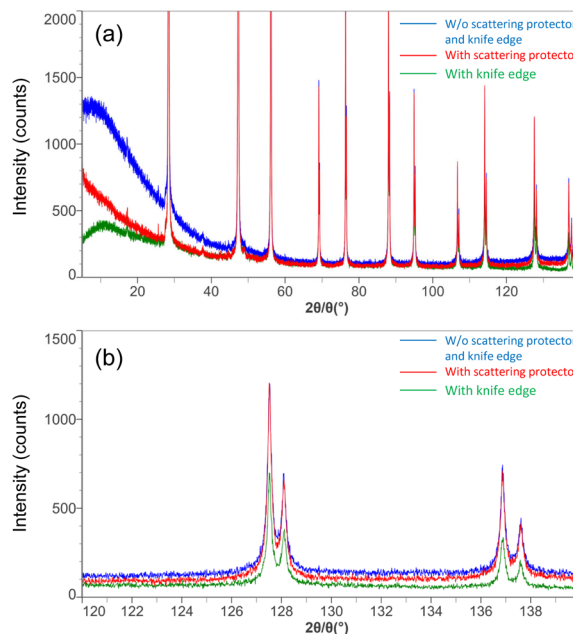


Fig. 6. Profiles measured with and without scattering protector and knife edge (a) $2\theta=5-140^\circ$, (b) $2\theta=120-140^\circ$ (Target metal: Cu, Sample: Si powder).

and the scattering protector is effective in the case of measurement on the high-angle side.

Generally, the knife edge is fixed at 2 mm above the sample surface. The measurable 2θ range depends on the size of the incident slit. It is necessary to check in advance that the knife edge is not blocking the diffracted X-rays.

(e) Receiving slit 1

The receiving slit 1 (RS1) is the slit used to block the scattered X-rays. This slit is also called the scattering slit. In the case of 0D measurement, the width of RS1 is generally selected to be the same as the incident slit. The detector plane for 1D measurement is wider than that of 0D measurement; therefore, the RS1 is selected such that it does not block the diffracted X-rays.

(f) $K\beta$ filter

In case of the $K\beta$ method, a thin metal film is inserted in the receiving optical system to decay the $K\beta$ line. When a Cu target is used, a $15\ \mu\text{m}$ or $23\ \mu\text{m}$ thick Ni film is used for the filter. When a $15\ \mu\text{m}$ Ni filter is used, the intensity ratio of $K\alpha$ to $K\beta$ line becomes 100 : 1, and with a $23\ \mu\text{m}$ Ni filter, the intensity ratio becomes 500 : 1. The relative intensity of the $K\beta$ line to the $K\alpha$ line decreases as the thickness of the filter increases; however, the absolute intensity of the $K\alpha$ line also decreases.

High-intensity peaks are detected when a sample with high crystallinity is measured. Therefore, it is preferred to use a thick filter to preventing the detection of diffraction peaks from the $K\beta$ line. On the other hand, when a sample with low crystallinity is measured, it is preferred to use a thin filter to increase the diffraction intensity.

(g) Receiving soller slit

A receiving soller slit determines the divergence angle in the longitudinal direction and prevents broadening of the diffraction peak by the vertical divergence effect (umbrella effect).

Figure 7 shows the relationship between the receiving soller slit and the umbrella effect. When the angular aperture of the soller slit is small, the umbrella effect reduces and the angular resolution improves. It is preferable to use a soller slit with a small angular aperture to separate adjacent diffraction peaks or for the measurement of crystallite size. When 5° incident and receiving soller slits are used, the diffraction intensity increases by 40% compared with the case when 2.5° soller slits are used. Therefore, the measurement time can be shortened.

(h) Receiving slit 2

The receiving slit 2 (RS2) determines the width of the irradiation area on the detector plane. When SmartLab Studio II is used as the control software and a 1D detector is used, there is no need to use a real slit for RS2. The 1D detector assumes the same role as a real slit by using part of the detector plane. This is called a virtual slit.

In the case of a 0D measurement, as the width of the receiving slit increases, the diffraction intensity

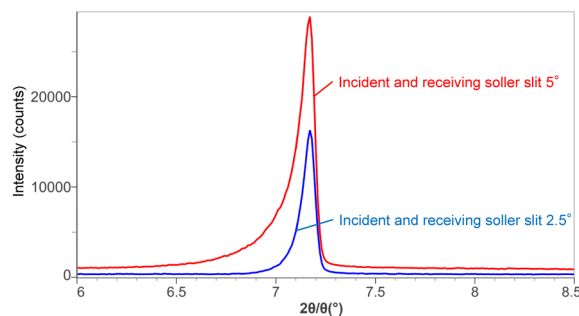


Fig. 7. Relationship between the soller slit and umbrella effect (Target metal: Cu, Sample: Si powder).

increases and the angular resolution decreases. Generally, a RS2 of 0.3 mm is used to compromise between peak intensity and angle resolution. Note that when a 1D detector, D/teX Ultra250, is used, a virtual slit of 0.375 mm is used.

In the case of a 1D measurement, different information on 2θ angles can be obtained simultaneously; therefore, the RS2 is usually kept open. Since the scan in a 1D measurement starts from the low angle side by a half of RS2, for measurements at small 2θ angle, there are cases where the diffracted X-rays are blocked by the direct beam stopper or incident X-rays are irradiated outside the sample.

Figure 8 shows the profiles measured with various RS2 sizes. When the RS2 is 10 mm or 20 mm, the diffracted X-rays on the low-angle side are blocked by the direct beam stopper. A pattern with the correct intensity ratio can be measured using a small RS2 width.

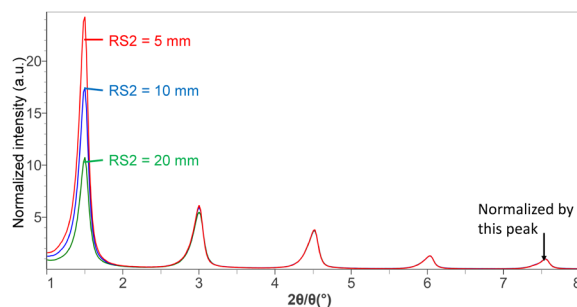


Fig. 8. Profiles measured with various sizes of RS2. Note that the profiles are normalized by the peak at $2\theta = 7.5^\circ$. (Target metal: Cu, Sample: silver behenate)

(i) Attenuator

Irradiating a detector with high-intensity X-rays may cause counting loss and detector troubles. In order to prevent that, it is necessary to use a thin metal film to attenuate the X-rays. An attenuator unit can change the attenuation ratio of the X-rays by switching between metal films having different thicknesses. When an automatic attenuator unit is used, the thickness of the metal film is selected automatically depending on the intensity of the detected X-rays, and measured profiles will automatically be combined. In TDI (Time Delay

Integration) mode, an automatic attenuator cannot be used. Therefore, you need to pay attention to avoid irradiating the detector with the direct X-ray beam in the case of a 1D scan.

5. Optical Systems Using a Mirror on the Incident Side

5.1. Parallel beam method

In the parallel beam method, X-rays are parallelized using a paraboloid multilayer mirror (CBO) and irradiated onto a sample (6). Because X-rays are monochromatized by the mirror, the $K\beta$ filter is unnecessary. The irradiated width is calculated using the width of the incident slit (IS) and incident angle (ω) as in Eq. (1).

$$\text{Irradiated width} = IS / \sin \omega \tag{Eq. (1)}$$

When a Cu target is used, the width of the irradiated beam from the CBO unit is approximately 0.8 mm; therefore, one should note that the width of the incident beam cannot be increased even if the width of the incident slit exceeds 0.8 mm.

Popular methods to detect X-rays are (a) 0D measurement using a parallel slit analyzer (PSA) and (b) 1D measurement using parallel beams.

(a) 0D measurement using a PSA

Figure 9 shows the schematic diagram of a measurement using a PSA. The PSA consists of stacked metal thin films in the 2θ direction. Because diffracted X-rays other than those at the target 2θ angle are removed, 0D measurement can be performed using the whole area of the detector and there is no effect of the specimen shape and eccentricity. The RS1 and RS2 are kept open so as not to block the diffracted X-rays.

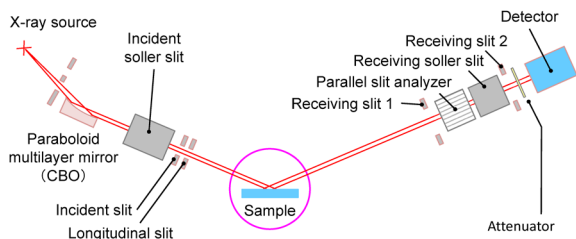


Fig. 9. The schematic diagram of a measurement using a PSA.

(b) 1D measurement using parallel beams

Figure 10 shows a schematic diagram of 1D measurement using a parallel beam. The sample is irradiated with parallelized X-rays and the diffraction angle of the diffracted X-rays is analyzed by the detector. The angular resolution depends on the width of the diffracted X-rays and improves as the width of the incident X-rays narrows. Figure 11 shows profiles measured by various widths of the incident slit. The width of the receiving slits is selected to block the scattered X-rays and so as not to block the diffracted X-rays. The optimal width of RS1 and RS2 depends

on the size of the area of the detector. In the case of the D/teX Ultra250, the RS1 and RS2 are set to 15 mm and 20 mm, respectively. In the case of the D/teX Ultra2, the RS1 and RS2 are set to 8 mm and 13 mm, respectively. Optimal widths of RS1 and RS2 are the same for the case of the BB method. Note that there is an effect of the eccentric error, because a parallel beam is used but a PSA is not used. This method is effective for the transmission method and for the reflection method with low background profiles in the low-angle region.

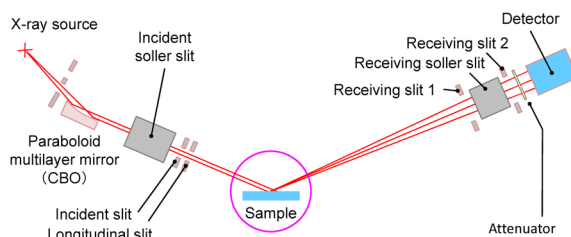


Fig. 10. A schematic diagram of a 1D measurement using parallel beams.

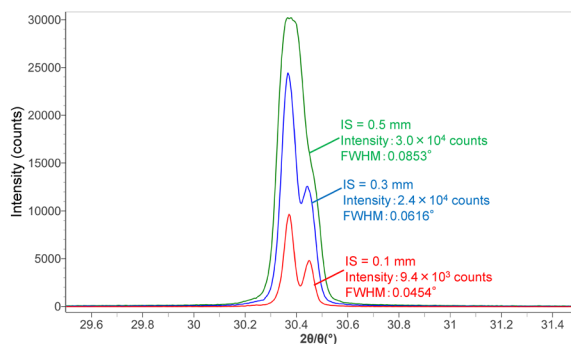


Fig. 11. Profiles measured with various widths of the incident slit (Target metal: Cu, Sample: LaB₆).

Figure 12 shows the dependence of the width of the incident slit measured by the transmission method using capillaries. As the incident slit widens, the intensity becomes higher but the angular resolution deteriorates. In the case of the transmission method, the angular resolution may improve using the focusing beam method (see below). Moreover, the angular resolution depends

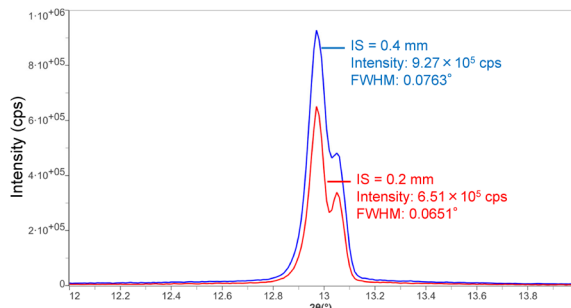


Fig. 12. Dependence of the width of the incident slit measured by the transmission method using capillaries (Target metal: Mo, Sample: Si, Radius of a capillary: 0.5 mm).

on the radius of the capillaries. The relationship between the radius of the capillaries and the angular resolution will be explained in the third article of the powder X-ray diffraction method.

5.2. Focusing beam method

Figure 13 shows a schematic diagram using the focusing beam method. X-rays converge through the CBO-E and irradiate the sample. The width of the incident slit is set to 0.7mm so as not to block the incident X-rays. Incident X-rays converge to 0.4mm at the sample position and 0.1mm at the detector position. Figure 14 shows profiles measured using the CBO-E or CBO. The measurement was performed by the transmission method using capillaries. Profiles with high intensity and high angular resolution can be obtained using the CBO-E unit. The width of the receiving slits is selected to block scattered X-rays and so as not to block the diffracted X-rays. Specifically, in the case of D/teX Ultra250, the RS1 and RS2 are set to 15mm and 20mm, respectively. In the case of the D/teX Ultra2, the RS1 and RS2 are set to 8mm and 13 mm, respectively.

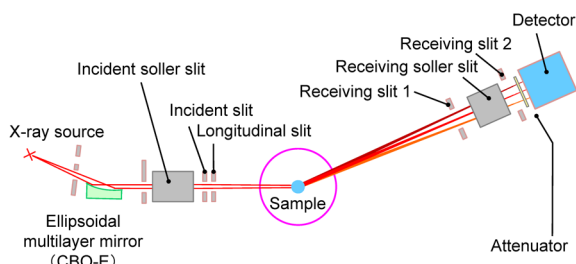


Fig. 13. A schematic diagram using the focusing beam method

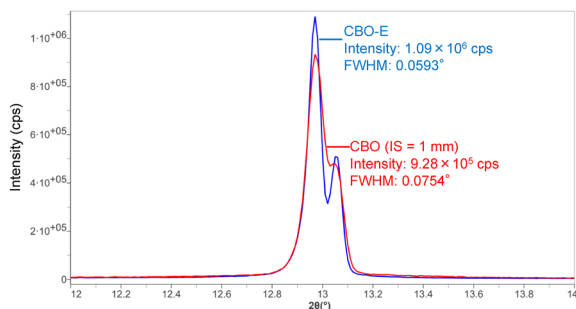


Fig. 14. Profiles measured using CBO-E or CBO by the transmission method using capillaries (Target metal: Mo, Sample: Si, Radius of a capillary: 0.5 mm).

6. Selection of the Energy Mode of the Detector

Various wavelengths of X-rays irradiate the detector other than the characteristic X-rays. When a semiconductor detector is used, unwanted X-rays can be reduced using the energy resolution of the detector. Detectors can have two energy modes: standard mode and fluorescence X-ray (XRF) reduction mode.

Figure 15 shows the energy distribution of the detector. This pattern was measured using diffraction from Si (111). The detectable energy range differs between the standard mode and XRF reduction mode. Figure 15 summarizes the energy ranges of the standard mode and XRF reduction mode when SmartLab Studio II is used as the control software.

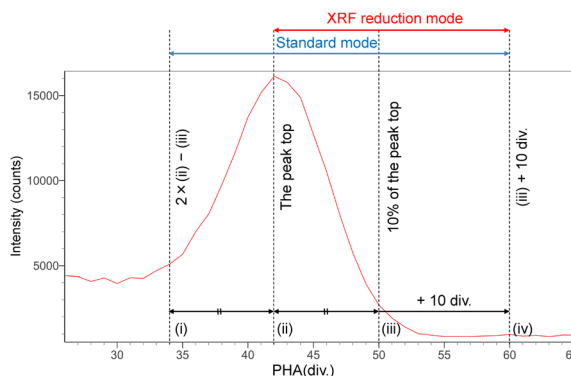


Fig. 15. The energy distribution of the detector and the energy ranges of the standard and XRF reduction mode (Target metal: Cu, Detector: D/teX Ultra250).

The minimum detectable energy in XRF reduction mode is higher than that with standard mode. Therefore, fluorescent X-rays can be reduced in XRF reduction mode and profiles with high P/B ratio can be obtained. The intensity of the diffracted X-rays in XRF reduction mode is half of that in standard mode because the $K\alpha$ line is also reduced; therefore, XRF reduction mode is not used for samples with low fluorescent X-rays.

Examples where XRF reduction mode is effective include the measurement of Fe-based or Mn-based samples using a Cu target and that of chromium steel using a Co target. Figure 16 shows the profiles of Fe_2O_3 measured using a Cu target. When XRF reduction mode is used, the P/B ratio improves.

Note that the residual ratio of the $K\beta$ line is high in XRF reduction mode; therefore, it is advisable to use a thick $K\beta$ filter and reduce the residual ratio of the $K\beta$ line.

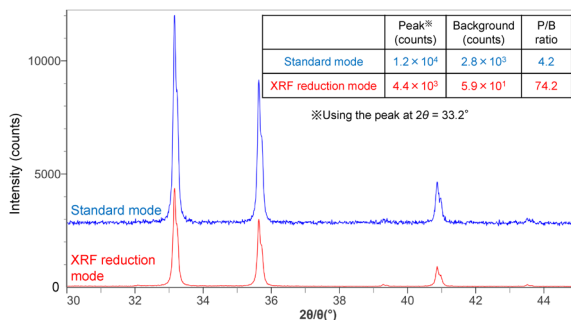


Fig. 16. The comparison between the standard and XRF reduction modes (Target metal: Cu, Sample: Fe_2O_3 , Detector: HyPix-3000).

7. Conclusion

In the second article of this series, the powder X-ray diffraction basic course, the selection of equipment configurations to obtain high-quality data has been explained. In the third article, sample preparation and scanning conditions to obtain high-quality data will be explained using concrete examples.

References

- (1) Yukiko Namatame: Rigaku Journal, **27** (2011), No. 1, 06–08.
- (2) Rigaku Journal, **27** (2011), No. 1, 20.
- (3) Takeshi Osakabe: Rigaku Journal, **33** (2017), No. 1, 15–19.
- (4) Yukiko Namatame: Rigaku Journal, **34** (2018), No. 2, 9–13.
- (5) Rigaku Journal, **34** (2018), No. 1, 30–31.
- (6) Toru Mitsunaga: Rigaku Journal, **25** (2009), No. 1, 7–12.